Organic Geochemistry 76 (2014) 167–172

Contents lists available at ScienceDirect

Organic Geochemistry

journal homepage: www.elsevier.com/locate/orggeochem

Flash pyrolysis of kerogens from algal rich oil shales from the Eocene Huadian Formation, NE China

Zhirong Zhang [a,b,c,*], John K. Volkman [b], Paul F. Greenwood [c,d,e], Wenxuan Hu [a], Jianzhong Qin [b], Tenger Borjigin [b], Changbo Zhai [b], Weixin Liu [b]

[a] School of Earth Sciences and Engineering, Nanjing University, Nanjing, Jiangsu 210023, China
[b] SINOPEC Key Laboratory of Petroleum Accumulation Mechanisms, Wuxi Institute of Petroleum Geology, SINOPEC, 2060 Lihu Road, Wuxi, Jiangsu 213126, China
[c] WA Organic and Isotope Geochemistry Centre, Department of Chemistry, Curtin University, GPO Box U1987, Perth, Western Australia 6845, Australia
[d] Centre for Exploration Targeting, The University of Western Australia, 35 Stirling Highway, Crawley, Western Australia 6009, Australia
[e] WA Biogeochemistry Centre, The University of Western Australia, 35 Stirling Highway, Crawley, Western Australia 6009, Australia

A R T I C L E I N F O

Article history:
Received 13 June 2014
Received in revised form 12 August 2014
Accepted 12 August 2014
Available online 22 August 2014

Keywords:
Huadian oil shale
Kerogen
Flash pyrolysis–GC–MS
Pyroprobe
Botryococcus braunii
Aromatic lycopane derivative

A B S T R A C T

The hydrocarbon composition of the kerogen fractions of two samples (HD-20 and HD-21) from oil shale layer 4 in the Eocene Huadian Formation, NE China were investigated by analytical flash pyrolysis (650 °C/10 s) followed by gas chromatography–mass spectrometry (Py–GC–MS). Organic petrography showed that the two kerogens were almost entirely derived from algal remains but contained very different algal maceral compositions, with 40% of the macerals in HD-20 being of macroalgal origin that were not present in HD-21. Py–GC–MS yielded high concentrations of *n*-alkanes from both kerogens, but with different molecular weight profiles due to the different algal contributors to the two kerogen samples. The hydrocarbon pyrolysates generated at 650 °C from HD-21 in which the green microalga *Botryococcus braunii* was identified showed a higher proportion of longer chain alkanes and alkenes presumably from cracking of the *botryococcus* algaenan. We also identified a C_{40} monoaromatic lycopane derivative, which was absent in the HD-20. The high hydrocarbon potential of both kerogens can be attributed to common microalgal sources, whereas the macroalgae, which is abundant in HD-20, makes only a minor contribution to the hydrocarbon products.

1. Introduction

Microalgae are the major source of organic matter in the organic rich Huadian oil shales (Xie et al., 2014) as found in many marine and lacustrine sediments (Volkman et al., 1998). Microalgae contain a variety of distinctive biomarkers (e.g. Volkman et al., 1998), which have been used as an efficient tool to study the paleoenvironment and degree of maturity of hydrocarbon source rocks and source of crude oils (Peters et al., 2005). Fossils believed to be related to the green microalga *Botryococcus* (Trebouxiophyceae) have been identified in sediments ranging from Precambrian to recent (Guy-Ohlson, 1992) and it has been recognized as a major source material for petroleum generation through geological time (Tissot and Welte, 1978; Glikson et al., 1989). *Botryococcus* has also been used as a paleoenvironmental indicator, especially for freshwater or brackish environments (Guy-Ohlson, 1992; Zhang et al., 2007).

The extant species *Botryococcus braunii* contains polymethylenic biopolymers (algaenans) and a remarkably diverse range of unusual compounds including highly branched C_{34}–C_{37} isoprenoid hydrocarbons called botryococcenes, a C_{40} lycopadiene and related oxygenated compounds that provide source diagnostic biomarker information (Maxwell et al., 1968; Metzger et al., 1991; Grice et al., 1998; Metzger and Largeau, 2005). Several taxonomically distinct races (A, B, L and S) of *B. braunii* can be distinguished by their hydrocarbon composition. Botryococcene related lipids are specific biomarkers biosynthesized by the race B of *B. braunii* (Maxwell et al., 1968), but they are not found in the algaenan. In contrast, the L race contains algaenan incorporating isoprenoid structures related to lycopadiene (Berthéas et al., 1999; structure modified by Salmon et al., 2009). Derenne et al. (1994) reported low amounts of a C_{40} monoaromatic hydrocarbon in pyrolysates of kerogens isolated from two recent sediments from a crater lake in Papua New Guinea and noted that one of these corresponded to the major compound identified in pyrolysates of the algaenan from

* Corresponding author at: School of Earth Sciences and Engineering, Nanjing University, Nanjing, Jiangsu 210023, China. Tel.: +86 510 68787516; fax: +86 510 83209327.

E-mail address: Zhangzr.syky@sinopec.com (Z. Zhang).

http://dx.doi.org/10.1016/j.orggeochem.2014.08.004
0146-6380/

B. braunii race L (Derenne et al., 1990). Adam et al. (2006) found the same compound in the extractable hydrocarbon fraction of the Messel oil shale (Eocene, Germany) and also attributed it to contributions from race L. A review of the reported geological occurrence of botryococcene- and lycopadiene-related lipids led Volkman (2014) to suggest that the biosynthetic pathways for the botryococcenes and lycopadiene in *Botryococcus* probably evolved during the Eocene (ca. 55 Ma).

The maceral composition of petroleum source rocks measured by petrographic analysis, traditionally using reflective, transmitted or fluorescence light sources, can often provide information about the major organic inputs and related depositional paleoenvironments (Breger and Brown, 1963; Tissot and Welte, 1978). Intact kerogens and asphaltenes, are intractable to many analytical methods, but can be degraded by chemical or thermal methods (Horsfield and Douglas, 1980; Largeau et al., 1986; Grice et al., 2003). Analytical pyrolysis followed by GC–MS analysis has been widely applied to characterize the hydrocarbon composition of kerogens and asphaltenes and the thermally generated molecules are often correlated with their corresponding free hydrocarbon or bitumen fractions isolated by solvent extractions (e.g., Larter et al., 1979; Solli and Leplat, 1986; Derenne et al., 1988, 1997; Greenwood et al., 1998, 2000; Liao et al., 2012; Tulipani et al., 2013; Zhang et al., 2014). Flash pyrolysis, in which very high amounts of thermal energy are applied to induce extensive fragmentation of macromolecular organic matter, has proven to be a rapid and simple method for structural characterization of kerogens often yielding high abundances of products amenable to GC–MS detection that are structurally representative of the whole fraction (Larter and Horsfield, 1993). Some of these hydrocarbon constituents may convey information relating to the organic precursors of fossil fuels or reflect their thermal maturity with respect to petroleum generation. Such information can assist oil correlation studies and help predict the economic scale of oil reserves (Philp and Gilbert, 1987).

In the present work, we compare the molecular composition of two kerogen samples isolated from the same unit within the organic rich lacustrine Huadian oil shale, based on flash Py–GC–MS analysis. These data are used to show that organic matter sources are dominated by algae as reflected by the presence of specific biomarkers and complemented by organic petrology (Xie et al., 2014).

2. Samples and methods

2.1. Geological setting and sample description

The Huadian Basin in Jilin Province, northeast China, is a fault-controlled basin filled with Eocene non-marine sediments (Wang et al., 2005). The Huadian Formation can be subdivided into Pyrite, Oil Shale and Carbonaceous Shale members (Sun et al., 2013). Macerals from microalgae, macroalgae and higher plants have been characterized by microscopic and chemical methods in oil shale layers 4, 5 and 6 of the Oil Shale Formation as defined by Sun et al. (2013). Full details can be found in Xie et al. (2014) who analyzed 22 samples from an underground mine in the Guanglangtou district by petrographic and bulk geochemical methods. Two samples (HD-20 and HD-21) having different maceral composition were selected from layer 4 (Xie et al., 2014) of the Huadian oil shale for geochemical analysis by Py–GC–MS to obtain molecular information representative of the different maceral compositions. The color of these rocks (and the kerogen fractions isolated from them) were notably different, with HD-21 more brown and HD-20 more black. The basic geochemical characters of the two kerogen fractions (Xie et al., 2014) are reported in Table 1 along with their maceral compositions.

2.2. Isolation of kerogen fraction

Finely ground oil shale rock samples (~50 g) were Soxhlet extracted with chloroform for 72 h, after which the extracted residue was continuously treated with 12 M HCl for about 12 h to remove carbonates. After washing with distilled water, the residue was treated with HF for another 12 h to remove silicate minerals (Guthrie and Pratt, 1994). The residue was then washed again (distilled water, x3), dried at ambient temperature and ultrasonicated in DCM for 30 min and finally dried at ambient temperature.

2.3. Flash Py–GC–MS

Flash pyrolysis of the kerogen samples were carried out with a CDS 5000 Pyroprobe equipped with an autosampler and linked to the GC inlet by a transfer line at 300 °C. Kerogen samples (0.5–1.5 mg) were loaded into quartz pyrolysis tubes for the flash pyrolysis. The two samples were each separately analyzed with pyrolysis temperatures of 650 °C and 800 °C to investigate the influence of pyrolysis temperature. The results from the 800 °C pyrolysis were substantially similar to those from 650 °C apart from a slight shift to lower carbon numbers and slightly higher content of alkadienes at 800 °C consistent with more extensive cracking at higher temperatures. Hence, we only present results from the 650 °C pyrolysis.

An Agilent 6890 GC coupled with a 5973 MSD was employed to analyze the pyrolysates. The injector was held at 300 °C with a split ratio of 50:1. Helium gas was used as carrier gas for both GC separation (1.2 ml/min) and for the transfer of pyrolysates. A DB-5MS capillary column (60 m length, 0.32 mm diam. and 0.32 μm film thickness) was employed for the GC separation. The GC oven was cooled with liquid CO_2 to an initial −20 °C (held for 1 min), and then increased at 8 °C/min to 40 °C and then at 4 °C/min to a final 320 °C held isothermally for 25 min. Mass spectra were acquired with 70 eV ionization and in full scan mode between 15 and 600 Da with an ion source temperature of 230 °C.

To minimize the influence of contamination and pyrolysis residues, a blank pyrolysis experiment was carried out before and after each pyrolysis using an empty quartz tube with a fast GC temperature program (50 °C to 325 °C at 20 °C/min).

3. Results and discussion

3.1. General characteristics of the isolated kerogens

Xie et al. (2014) showed that oil shales from layer 4 have the highest TOC values (24.9–39.6%), hydrocarbon generation potential (S2 values from Rock–Eval analysis were 88.2–59 mg HC/g rock) as well as high Hydrogen Index (HI value 230–887 mg HC/g TOC) and low Oxygen Index (OI value). Xie et al. (2014) characterized the oil shales as low maturity Type I kerogen (average T_{max} = 442 °C). Sulfur contents were very low (0.01–0.31%) and typical of lacustrine sediments.

Bulk organic geochemical and petrographic information for HD-20 and HD-21 are listed in Table 1. Although the HD-20 sample has a 10% higher TOC value than HD-21, the latter has about 65 mg HC/g rock more hydrocarbon generation potential than the former and almost double the HI value (Table 1). Differences in the organic maceral composition and hydrocarbon generating properties imply differences in molecular structure that would be expected to translate into different pyrolysate compositions.

Lamalginite dominates the macerals in both HD-20 and HD-21 (50.9% and 67.6% respectively; Table 1). HD-21 also contains a high proportion of telalginite (30.0%) whereas this comprises only 5.6% of the macerals in HD-20. Benthic macroalginite (of presumed

Table 1
Bulk organic geochemical and petrographic information for kerogens of HD-20 and HD-21.

No.	Layer	TOC (%)	C/S	S2 (mg HC/g rock)	Tmax (°C)	HI	OI	Alginate (%)		Benthic	Vitrinite	Inertinite
								Telalginite	Lamalginite	Macroalginite (%)	Detrovitrinite (%)	Funginite (%)
HD-20	4	39.6	63.9	194	436	490	21	5.6	50.9	43.0	–	0.5
HD-21	4	29.8	119	259	446	869	7	30.3	67.7	–	2.4	–

origin from red macroalgae) comprises 43% of the macerals in HD-20, but none was identified in HD-21.Macerals from higher plants were very minor constituents and detrovitrinite was only detected in HD-21, and even there it was only 2.4%. These samples thus provide excellent examples of organic rich shales where the organic matter is almost completely of algal origin, but with differing proportions from microalgae and macroalgae. The main microalgal contributors include diatoms, which are associated with the lamalginite, whereas the telalginite is associated with the green colonial microalga *B. braunii* as well as acritarchs *Leisphaeridia* and *Micrhystridium* (Xie et al., 2014).

3.2. Hydrocarbon pyrolysates

The total ion current (TIC) chromatograms from Py–GC–MS of HD-20 and HD-21 kerogens at 650 °C are shown in Fig. 1. Both display a dominant homologous distribution of *n*-alkane/*n*-alk-1-ene doublets from C_6 extending to beyond C_{30}. The *n*-alk-1-enes start to co-elute with *n*-alkanes from *n*-C_{29}. The chromatograms of aliphatic hydrocarbons show a minimum at C_9 for HD-20, whereas for HD-21 the minimum was at C_{15}. Note however, that the relative abundance of shorter chain hydrocarbons is overemphasized by the peak heights, but this is not so apparent when peak areas are considered. High yields of aliphatic rich hydrocarbon products have also been commonly obtained from the pyrolysis of type I kerogens (Larter et al., 1977; Horsfield, 1989) and these *n*-alkane/alkene distributions are similar to those previously reported from lacustrine algal dominated kerogens (e.g., Derenne et al., 1994; Grice et al., 2003), but quite different from many kerogens of marine origin, which typically show a maximum around *n*-C_{13} and a relatively low abundance of C_{20}+ compounds (Gray et al., 1991).

Below *n*-C_{20}, the aliphatic hydrocarbons distributions of the kerogen pyrolysates showed quite similar abundances, but the HD-21 pyrolysates had a distinctly higher proportion of HMW *n*-aliphatics (*n*-C_{20}+) compared to those from HD-20 (Table 2). This suggests that the two kerogens have similar contributors of short to middle chain *n*-aliphatics, but HD-21 contains abundant precursors of longer chain hydrocarbons. The high yield of HMW *n*-aliphatics from the HD-21 kerogen likely reflects the higher proportion of telalginite in this sample since the proportions of lamalginite are very similar in the two rocks (Table 1). It is significant that this telalginite is associated with *Botryococcus,* which is known to produce large quantities of long chain hydrocarbons as well as containing long chain polymethylenic algaenan (Derenne et al., 1994; Volkman, 2014 and references therein). We can discount the possibility of terrigenous macerals as a source of these long chain alkanes given the very low abundance of vitrinite macerals in HD-21 (Table 1).

Little has been reported on the analytical pyrolytic behavior of macroalgae, but a high content of N or O containing compounds appears to be a common feature (Ross et al., 2009; Ferrera-Lorenzo et al., 2014) and may provide possible bio-precursor of source rocks (Cao et al., 2009). Their relatively low hydrocarbon yield is due to a typically very low lipid content and absence of algaenans (Harwood and Jones, 1989; Nelson et al., 2002). The very similar aliphatic hydrocarbon dominated profiles obtained from the flash pyrolysis of HD-20 and HD-21 indicates that the high proportion of benthic macroalginite in HD-20 (43%) does not contribute significantly to the hydrocarbons generated on pyrolysis.

Variations in the *n*-alkanes to *n*-alkenes ratio in pyrolysates of organic matter have been widely reported (Coburn et al., 1978 and references therein). Here the ratio of *n*-alkanes to *n*-alkenes increases with carbon number (Fig. 2). Prist-1-ene is a ubiquitous product from algal material flash pyrolysis and its source is usually attributed to the phytyl side chain of chlorophyll (Larter et al., 1979; Höld et al., 2001). The abundance of prist-1-ene (ca. 0.6 with respect to *n*-heptadecane for HD-20 and 0.3 for HD-21, Fig. 1) is consistent with low thermal maturity (van Graas et al., 1981) and multiple sources. The low abundance of other isoprenoids is surprising since a variety of isoprenoids can be produced by pyrolysis of algaenans from *B. braunii* (Derenne et al., 1994, 1997).

3.3. Aromatic hydrocarbon distributions

Relatively low amounts of aromatic hydrocarbons were detected in the kerogen pyrolysates and the dominant component

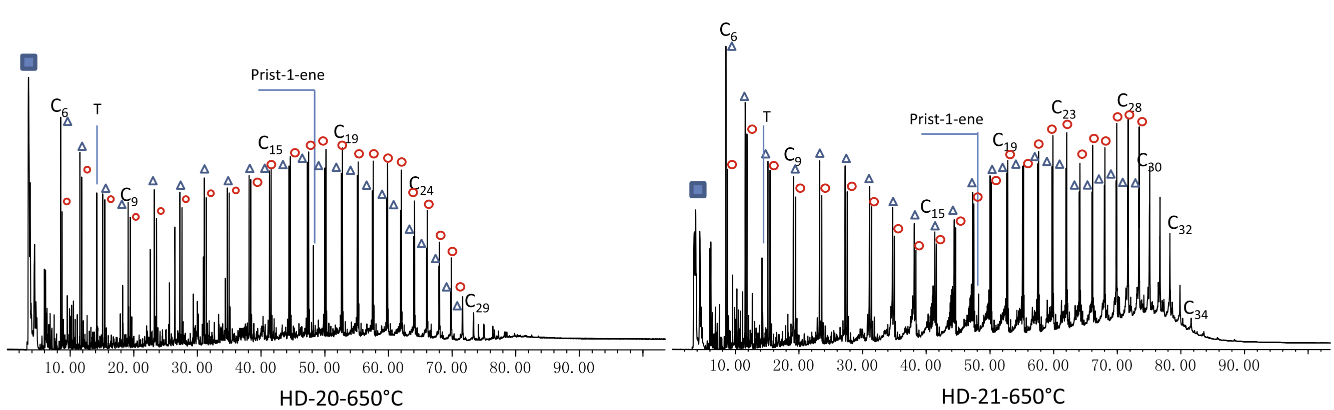

Fig. 1. TICs of pyrolysates of HD-20 and HD-21 kerogens at 650 °C; squares: unresolved compounds; circles: *n*-alkanes; triangles: *n*-alkenes; T = toluene; Cn = alkane/ene doublets.

Table 2
Saturate and aromatic ratios for kerogen pyrolysates of HD-20 and HD-21.

Ratios	HD-20	HD-21
Benzene/total monoaromatics	0.19	0.24
Toluene/total monoaromatics	0.45	0.44
Toluene/n-C_8 (alkane + alkene)	2.56	1.02
C_{20}–C_{29} (aliphatic)/C_6–C_{29} (aliphatic)	0.34	0.42

Ratios were calculated from peak areas in the mass fragmentograms for m/z 78 (benzene), m/z 91 (monoaromatics), m/z 85 (n-alkanes) and m/z 83 (n-alkenes); aliphatics = n-alkanes + n-alkenes.

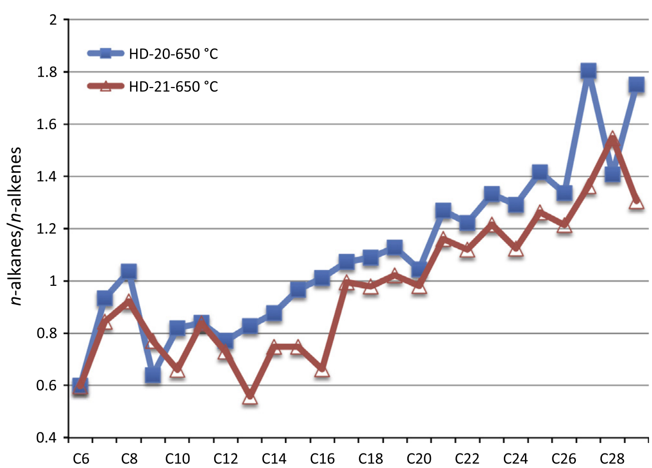

Fig. 2. n-Alkane/ene ratios vs. carbon number in the pyrolysates of HD-20 and HD-21.

was toluene (Fig. 1). Methyl naphthalenes were minor compounds and higher polycyclic aromatic hydrocarbons (PAHs) were negligible. The proportion of aromatics from HD-20 was higher than from HD-21 (cf. T/n-C_8). Plant-derived macerals such as vitrinite typically show high proportions of aromatics in pyrolysates (Solli and Leplat, 1986; Yoshioka and Takeda, 2004), but PAHs are usually the major compounds detected. It is clear that plant sources make little contribution to the aromatics found in the Huadian pyrolysates. For a long time, the relationship between the aromatic hydrocarbon distributions liberated from algae-sourced organic matter has been unclear, but it has been reported that certain algaenans such as those found in dinoflagellates (Kokinos et al., 1998) could generate aromatic rich pyrolysates. Kokinos et al. (1998) showed that aromatic and furanic products dominate over aliphatics in the pyrolysis of a dinoflagellate whilst Derenne et al. (1996) showed PAHs dominated the pyrolysate of a marine microalga *Chlorella marina*. However, the pyrolysis products of those two organisms were quite different from those reported here. Our data showed that algal derived, lacustrine kerogens can produce considerable amounts of simple aromatics such as benzene, toluene and HMW alkylbenzenes on pyrolysis. Aliphatic algaenans can produce aromatic compounds upon pyrolysis through cyclisation and further aromatization reactions as demonstrated by pyrolysis of polyethylene (e.g. Jung et al., 2010).

Fig. 3 shows the distributions of aromatic hydrocarbons in the pyrolysates. The ratios of benzene and toluene separately calculated relative to total monoaromatics for HD-20 and HD-21 are 0.19 and 0.24, and 0.45 and 0.44, respectively. The 2.56 value for toluene/n-C_8 ratio of HD-20 sample was distinctly higher than the 1.02 value for HD-21 (Table 2). No S-bonded compounds, such as DBT, were detected in either sample which is consistent with their low total sulfur content (Xie et al., 2014).

3.4. B. braunii biomarkers

Botryococcene derivatives represent highly diagnostic markers for *B. braunii* in sediments and petroleum but they are restricted to the race B of *B. braunii*, and are not biosynthesized by races A, L or S (Metzger and Largeau, 2005; Volkman, 2014). Race L produces a diagnostic C_{40} isoprenoid diene (lycopadiene), but this is rarely found in sediments. However, Adam et al. (2006) reported a C_{40} monoaromatic lycopane derivative in the extractable hydrocarbons of the Messel oil shale and proposed that it can be used as a specific biomarker for race L in sediments deposited under freshwater and/or brackish conditions (Derenne et al., 1994; Grice et al., 1998; Adam et al., 2006; Volkman, 2014). The lipids from *B. braunii* race L appear to be restricted to sediments from the Eocene or younger (Derenne et al., 1994; Grice et al., 1998; Fuhrmann et al., 2004; Adam et al., 2006; Volkman, 2014), although there is one report of a C_{40} monoaromatic hydrocarbon apparently related to lycopane in a Permian sediment (Kluska et al., 2013) and the same series of C_{40} hydrocarbons and ketone identified in the algaenan of the L race was reported in the pyrolysate of a Cenomanian black shale (Salmon et al., 1997). In neither case could an origin from *Botryococcus* be confirmed due to the lack of morphological remains and a source other than *Botryococcus* is possible (Volkman, 2014).

A specific C_{40} biomarker of race L *B. braunii* was identified in the pyrolysate of HD-21 in which *B. braunii* has been petrographically identified (Xie et al., 2014). Fig. 4 shows the partial TIC and m/z 119 mass fragmentogram as well as its mass spectrum. This biomarker eluted after n-C_{34} and has a molecular ion at 554 Da and a major fragment ion at 119 Da which matches well with published data (Derenne et al., 1990; Adam et al., 2006). Despite its low abundance it could be readily identified.

It has been suggested the formation of the C_{40} aromatic hydrocarbon takes place during early diagenesis from lycopadiene related precursors biosynthesized by *B. braunii* race L formed from functionalized precursors (lycopanerols) by isomerization/cyclisation reactions (Adam et al., 2006). Our results and those of Derenne et al. (1994) show that small amounts also can be released by thermal cleavage directly from kerogen macromolecules. Analysis of the extractable hydrocarbons from the oil shale also revealed the presence of the C_{40} monoaromatic together with small amounts of lycopadienes and lycopane (unpublished data). These results show for the first time that the *B. braunii* populations in the Huadian oil shale includes race L, although we cannot discount other races also being present. Pyrolysis of kerogen from the B race does not liberate botryococcanes/botryococcenes so this cannot be used to indicate the presence or absence of this race (Largeau et al., 1986; Derenne et al., 1994). However, we did not find botryococcane in the extractable lipids from these rocks (unpublished data) so it may be that this race was not present in the depositional environment.

3.5. n-Alkadienes

The pyrolysate of HD-21 was more complex than that of HD-20 (Fig. 1), and included an unresolved complex mixture hump that was more obvious in the HMW (C_{25}–C_{35}) zone. A series of n-alkadienes were detected by pyrolysis of both kerogens. The n-alkadienes elute just before corresponding n-alkanes and were readily distinguished since the fragment ion at m/z 67 which was stronger than in the mass spectra of n-alk-1-enes. After n-C_{21}, they start to co-elute with n-alk-1-enes (chromatograms not shown). Abundant n-alkadienes have been reported in the pyrolysates of the resistant biopolymers of races A, B and L of *B. braunii* (Derenne et al., 1994). The abundance for n-alkadienes dropped quickly with increasing number of carbons.

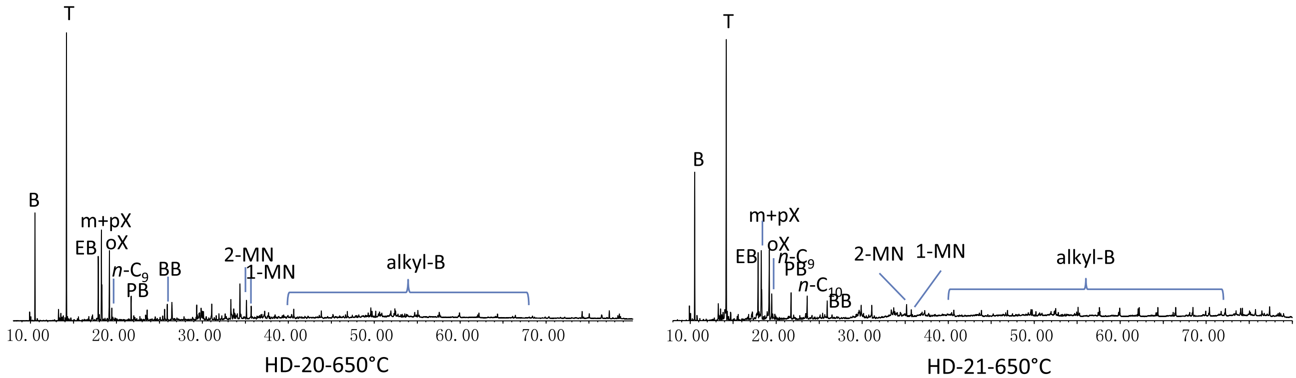

Fig. 3. Combined m/z 78 + 91 + 128 + 142 mass fragmentogram showing the aromatic hydrocarbon distributions in pyrolysates of kerogens of HD-20 and HD-21. B = benzene; T = toluene; EB = ethylbenzene; m + p + oX = m + para + ortho-xylene; PB = propyl benzene; BB = butylbenzene; MN = methyl naphthalene; alkyl-B = long chain alkyl benzenes.

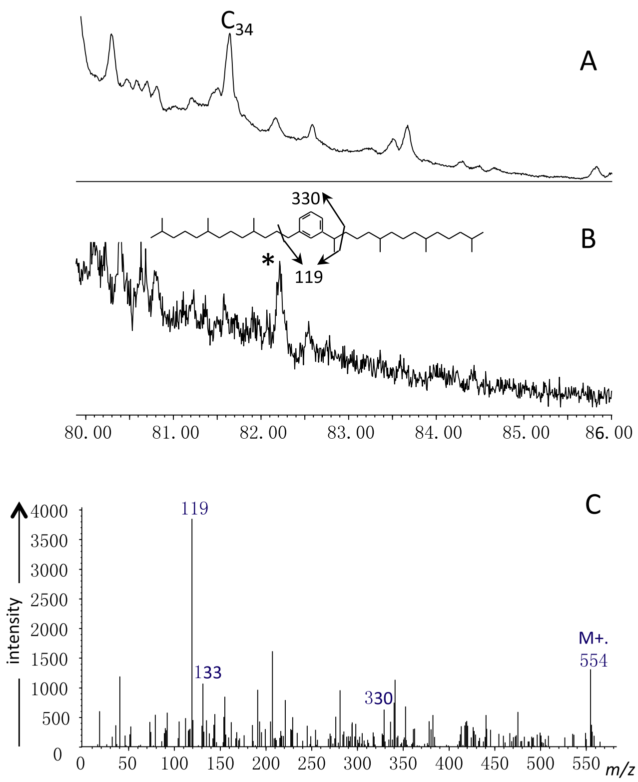

Fig. 4. Partial TIC (a) and m/z 119 mass chromatogram (b) and mass spectrum (c) of C_{40} monoaromatic biomarker in 650 °C pyrolysate of HD-21.

4. Conclusions

Pyrolysis of kerogens isolated from two oil shale samples from the Huadian Formation has enabled us to determine the hydrocarbon compositions of kerogens that are predominantly derived from lacustrine algae. Both samples produce a wide range of saturated and unsaturated n-aliphatics from C_5 to at least C_{30} reflecting the contribution from microalgae present in the lamalginite. The proportion of chain lengths > n-C_{25} rapidly decreases in the HD-20 pyrolysate, but in HD-21 there is an enhanced contribution of these chain lengths due to the contribution from pyrolysis of the telalginite. A major contributor to this is algaenan from the colonial green alga *B. braunii*. The high content of macerals from a benthic macroalga in HD-20 makes very little contribution to the pyrolysate hydrocarbons and confirms that macroalgae are not major contributors to the hydrocarbon potential in these shales as suggested by Xie et al. (2014). The low content and similarity of aromatic hydrocarbons in the pyrolysates indicates that LMW aromatics can be generated from algal kerogens, but the absence of PAHs is consistent with the very low contents of vitrinite present. The presence of a diagnostic C_{40} monoaromatic lycopane derivative in the pyrolysate of the kerogen of HD-21 shows that the population of *B. braunii* includes race L.

Acknowledgements

The authors acknowledge the financial support of SINOPEC Key Laboratory of Petroleum Accumulation Mechanisms open funds Project (No. 33550007-12-ZC0613-0049), SINOPEC Scientific Development Department Project (P13089) and China Major Science 973 Projects (No. 2012CB214801). Geoff Chidlow and Xiaomin Xie are thanked for the Pyroprobe GC-MS and maceral analysis, respectively. We thank the journal associate editor, Dr. Clifford Walters and two reviewers Drs Sylvie Derenne and Ling Gao for their helpful comments which improved the manuscript.

Associate Editor—**Cliff Walters**

References

Adam, P., Schaeffer, P., Albrecht, P., 2006. C_{40} monoaromatic lycopane derivatives as indicators of the contribution of the alga *Botryococcus braunii* race L to the organic matter of Messel oil shale (Eocene, Germany). Organic Geochemistry 37, 584–596.

Berthéas, O., Metzger, P., Largeau, C., 1999. A high molecular weight complex lipid, aliphatic polyaldehyde tetraterpenediol polyacetal from *Botryococcus braunii* (L race). Phytochemistry 50, 85–96.

Breger, I.A., Brown, A., 1963. Distribution and types of organic matter in a barred marine basin. Transactions of the New York Academy of Sciences 25, 741–755.

Cao, J., Bian, L., Hu, K., Liu, Y., Yang, S., Wang, L., Chen, Y., Peng, X., 2009. Benthic macro red alga: a new possible bio-precursor of Jurassic source rocks in the northern Qaidam Basin, NW China. Science China: Earth Sciences 52, 647–654.

Coburn, T.T., Bozak, R.E., Clarkson, J.E., Campbell, J.H., 1978. Correlation of shale oil 1-alkene/n-alkane ratios with process yield. Analytical Chemistry 50, 958–962.

Derenne, S., Largeau, C., Casadevall, E., Connan, J., 1988. Comparison of torbanites of various origins and evolutionary stages. Bacterial contribution to their formation. Cause of the lack of botryococcane in bitumens. Organic Geochemistry 12, 43–59.

Derenne, S., Largeau, C., Casadevall, E., Sellier, N., 1990. Direct relationship between the resistant biopolymer and the tetraterpenic hydrocarbon in the lycopadiene race of *Botryococcus braunii*. Phytochemistry 29, 2187–2192.

Derenne, S., Largeau, C., Behar, F., 1994. Low polarity pyrolysis products of Permian to Recent *Botryococcus*-rich sediments: first evidence for the contribution of an isoprenoid algaenan to kerogen formation. Geochimica et Cosmochimica Acta 58, 3703–3711.

Derenne, S., Largeau, C., Berkaloff, C., 1996. First example of an algaenan yielding an aromatic-rich pyrolysate: possible geochemical implications on marine kerogen formation. Organic Geochemistry 24, 617–627.

Derenne, S., Largeau, C., Hetenyi, M., Bruknerwein, A., Connan, J., Lugardon, B., 1997. Chemical structure of the organic matter in a Pliocene maar-type shale – implicated *Botryococcus* race strains and formation pathways. Geochimica et Cosmochimica Acta 61, 1879–1889.

Ferrera-Lorenzo, N., Fuente, E., Suárez-Ruiz, I., Gil, R.R., Ruiz, B., 2014. Pyrolysis characteristics of a macroalgae solid waste generated by the industrial production of Agar-Agar. Journal of Analytical and Applied Pyrolysis 105, 209–216.

Fuhrmann, A., Horsfield, B., Lopez, J.F., Hu, L.G., Zhang, Z.W., 2004. Organic facies, depositional environment and petroleum generating characteristics of the lacustrine Shahejie Formation, Es-4 Member, Western Depression, Liaohe Basin (NE China). Journal of Petroleum Geology 27, 27–45.

Glikson, M., Lindsay, K., Saxby, J., 1989. *Botryococcus* – a planktonic green alga, the source of petroleum through the ages: transmission electron microscopical studies of oil shales and petroleum source rocks. Organic Geochemistry 14, 595–608.

Gray, N.R., Lancaster, C.J., Gethner, J., 1991. Chemometric analysis of pyrolysate compositions – a model for predicting the organic-matter type of source rocks using pyrolysis–gas chromatography. Journal of Analytical and Applied Pyrolysis 20, 87–106.

Greenwood, P.F., George, S.C., Hall, K., 1998. Applications of laser micropyrolysis–gas chromatography–mass spectrometry. Organic Geochemistry 29, 1075–1089.

Greenwood, P.F., Arouri, K.R., George, S.C., 2000. Tricyclic terpenoid composition of *Tasmanites* kerogen as determined by pyrolysis GC-MS. Geochimica et Cosmochimica Acta 64, 1249–1263.

Grice, K., Schouten, S., Nissenbaum, A., Charrach, J., Sinninghe Damsté, J.S., 1998. A remarkable paradox: sulfurised freshwater algal (*Botryococcus braunii*) lipids in an ancient hypersaline euxinic ecosystem. Organic Geochemistry 28, 195–216.

Grice, K., Schouten, S., Blokker, P., Derenne, S., Largeau, C., Nissenbaum, A., Sinninghe Damsté, J.S., 2003. Structural and isotopic analysis of kerogens in sediments rich in free sulfurised *Botryococcus braunii* biomarkers. Organic Geochemistry 34, 471–482.

Guthrie, J.M., Pratt, L.M., 1994. Geochemical indicators of depositional environment and source-rock potential for the Upper Ordovician Maquoketa Group, Illinois Basin. American Association of Petroleum Geologists Bulletin 78, 744–757.

Guy-Ohlson, D., 1992. *Botryococcus* as an aid in the interpretation of palaeoenvironment and depositional processes. Review of Palaeobotany and Palynology 71, 1–15.

Harwood, J.L., Jones, A.L., 1989. Lipid metabolism in algae. In: Callow, J.A. (Ed.), Advances in Botanical Research, vol. 16. Academic Press, London, pp. 1–53.

Höld, I.M., Schouten, S., Van der Gaast, S.J., Sinninghe Damsté, J.S., 2001. Origin of prist-1-ene and prist-2-ene in kerogen pyrolysates. Chemical Geology 172, 201–212.

Horsfield, B., 1989. Practical criteria for classifying kerogens: some observations from pyrolysis–gas chromatography. Geochimica et Cosmochimica Acta 53, 891–901.

Horsfield, B., Douglas, A.G., 1980. The influence of minerals on the pyrolysis of kerogens. Geochimica et Cosmochimica Acta 44, 1119–1131.

Jung, S.-H., Cho, M.-H., Kang, B.-S., Kim, J.-S., 2010. Pyrolysis of a fraction of waste polypropylene and polyethylene for the recovery of BTX aromatics using a fluidized bed reactor. Fuel Processing Technology 91, 277–284.

Kluska, B., Rospondek, M.J., Marynowski, L., Schaeffer, P., 2013. The Werra cyclotheme (Upper Permian, fore-sudetic monocline, Poland): insights into fluctuations of the sedimentary environment from organic geochemical studies. Applied Geochemistry 29, 73–91.

Kokinos, J.P., Eglinton, T.I., Goñi, M.A., Boon, J.J., Martoglio, P.A., Anderson, D.M., 1998. Characterization of a highly resistant biomacromolecular material in the cell wall of a marine dinoflagellate resting cyst. Organic Geochemistry 28, 265–288.

Largeau, C., Derenne, S., Casadevall, E., Kadouri, A., Sellier, N., 1986. Pyrolysis of immature Torbanite and of the resistant biopolymer (PRB A) isolated from extant alga *Botryococcus braunii*. Mechanism of formation and structure of torbanite. Organic Geochemistry 10, 1023–1032.

Larter, S.R., Horsfield, B., 1993. Determination of structural components of kerogen by the use of analytical pyrolysis methods. In: Engel, M., Macko, S. (Eds.), Organic Geochemistry. Plenum Press, New York, pp. 271–287.

Larter, S.R., Horsfield, B., Douglas, A.G., 1977. Pyrolysis as a possible means of determining the petroleum generating potential of sedimentary organic matter. In: Jones, C.E.R., Cramers, C.A. (Eds.), Analytical Pyrolysis. Elsevier, pp. 189–202.

Larter, S.R., Solli, H., Douglas, A.G., de Lange, F., de Leeuw, J.W., 1979. Occurrence and significance of prist-1-ene in kerogen pyrolysates. Nature 279, 405–408.

Liao, Y., Fang, Y., Wu, L., Geng, A., Hsu, C.S., 2012. The characteristics of the biomarkers and $\delta^{13}C$ of *n*-alkanes released from thermally altered solid bitumens at various maturities by catalytic hydropyrolysis. Organic Geochemistry 46, 56–65.

Maxwell, J.R., Douglas, A.G., Eglinton, G., McCormick, A., 1968. The Botryococcenes—hydrocarbons of novel structure from the alga *Botryococcus braunii*, Kützing. Phytochemistry 7, 2157–2171.

Metzger, P., Largeau, C., 2005. *Botryococcus braunii*: a rich source for hydrocarbons and related ether lipids. Applied Microbiology and Biotechnology 66, 486–496.

Metzger, P., Largeau, C., Casadevall, E., 1991. Lipids and macromolecular lipids of the hydrocarbon-rich microalga *Botryococcus braunii*. Chemical structure and biosynthesis. Geochemical and biotechnological importance. In: Herz, W., Kirby, G.W., Steglich, W., Tamm, C. (Eds.), Progress in the Chemistry of Organic Natural Products. Springer-Verlag, Vienna, pp. 1–70.

Nelson, M.M., Phleger, C.F., Nichols, P.D., 2002. Seasonal lipid composition in macroalgae of the northeastern Pacific Ocean. Botanica Marina 45, 58–65.

Peters, K.E., Walters, C.C., Moldowan, J.M., 2005. The Biomarker Guide. Biomarkers and Isotopes in the Environment and Human History, vol. 1. Cambridge University Press, Cambridge.

Philp, R.P., Gilbert, T.D., 1987. A review of biomarkers in kerogens as determined by pyrolysis–gas chromatography and pyrolysis–gas chromatography–mass spectrometry. Journal of Analytical and Applied Pyrolysis 11, 93–108.

Ross, A.B., Anastasakis, K., Kubacki, M., Jones, J.M., 2009. Investigation of the pyrolysis behaviour of brown algae before and after pre-treatment using PY–GC/MS and TGA. Journal of Analytical and Applied Pyrolysis 85, 3–10.

Salmon, V., Derenne, S., Largeau, C., Beaudoin, B., Bardoux, G., Mariotti, A., 1997. Kerogen chemical structure and source organisms in a Cenomanian organic-rich black shale (Central Italy) – Indications for an important role of the "sorptive protection" pathway. Organic Geochemistry 27, 423–438.

Salmon, E., Behar, F., Lorant, F., Hatcher, P.G., Metzger, P., Marquaire, P.-M., 2009. Thermal decomposition processes in algaenan of *Botryococcus braunii* Race L. Part 1: experimental data and structural evolution. Organic Geochemistry 40, 400–415.

Solli, H., Leplat, P., 1986. Pyrolysis–gas chromatography of asphaltenes and kerogens from source rocks and coals – a comparative structural study. Organic Geochemistry 10, 313–329.

Sun, P.C., Sachsenhofer, R.F., Liu, Z.J., Strobl, S.A.I., Meng, Q.T., Liu, R., Zhen, Z., 2013. Organic matter accumulation in the oil shale- and coal-bearing Huadian Basin (Eocene, NE China). International Journal of Coal Geology 105, 1–15.

Tissot, B., Welte, D., 1978. Petroleum Formation and Occurrence. Springer, Berlin, Heidelberg and New York.

Tulipani, S., Grice, K., Greenwood, P., Schwark, L., 2013. A pyrolysis and stable isotopic approach to investigate the origin of methyltrimethyltridecylchromans (MTTCs). Organic Geochemistry 61, 1–5.

van Graas, G., de Leeuw, J.W., Schenck, P.A., Haverkamp, J., 1981. Kerogen of Toarcian shales of the Paris Basin. A study of its maturation by flash pyrolysis techniques. Geochimica et Cosmochimica Acta 45, 2465–2474.

Volkman, J.K., 2014. Acyclic isoprenoid biomarkers and evolution of biosynthetic pathways in green algae of the genus *Botryococcus*. Organic Geochemistry 75, 36–47.

Volkman, J.K., Barrett, S.M., Blackburn, S.I., Mansour, M.P., Sikes, E.L., Gelin, F., 1998. Microalgal biomarkers: a review of recent research developments. Organic Geochemistry 29, 1163–1179.

Wang, Y., Liu, Z., Jin, H., Zhang, H., Zhang, J., 2005. Sedimentary characteristics of oil shale deposit of the Huadian Formation of Paleogene in Huadian Basin. Journal of Jiling University (Earth Science Edition).

Xie, X., Volkman, J.K., Qin, J., Borjigin, T., Bian, L., Zhen, L., 2014. Petrology and hydrocarbon potential of microalgal and macroalgal dominated oil shales from the Eocene Huadian Formation, NE China. International Journal of Coal Geology 124, 36–47.

Yoshioka, H., Takeda, N., 2004. Analysis of organic compounds in coal macerals by infrared laser micropyrolysis. Journal of Analytical and Applied Pyrolysis 71, 137–149.

Zhang, Z., Metzger, P., Sachs, J.P., 2007. Biomarker evidence for the co-occurrence of three races (A, B and L) of *Botryococcus braunii* in El Junco Lake, Galápagos. Organic Geochemistry 38, 1459–1478.

Zhang, Z., Hu, W., Song, X., Zhang, C., Zhang, Q., Jin, J., 2014. A comparison of results from two different flash pyrolysis methods on a solid bitumen sample. Organic Geochemistry 69, 36–41.